

An Industrial Case Study - Control of BeoSound 9000 Sledge System

Zhenyu Yang

Department of Computer Science and Engineering

Aalborg University Esbjerg

Niels Bohrs Vej 8

DK-6700, Denmark

Tel: +45 79 12 76 08

Fax: +45 79 12 77 10

Email: yang@cs.aaue.dk

ACKNOWLEDGMENTS

Thanks go to

- Former students - B. B. Nørregaard, K. D. Rasmussen, L. H. Andreasen, J. Laas, L. H.P. Andersen for their preliminary investigations...
- H. F. Mikkelsen from Bang & Olufsen A/S.
- Gerulf Pedersen from AAUE.

Contents

1. Introduction
2. Mathematical Model of the considered Sledge System
3. Parameter Identification
4. Simulation and Model Validation
5. Control Design and Test Results
6. Conclusions

1. Introduction



Figure 1: BeoSound 9000 on its designated stand and its surface look

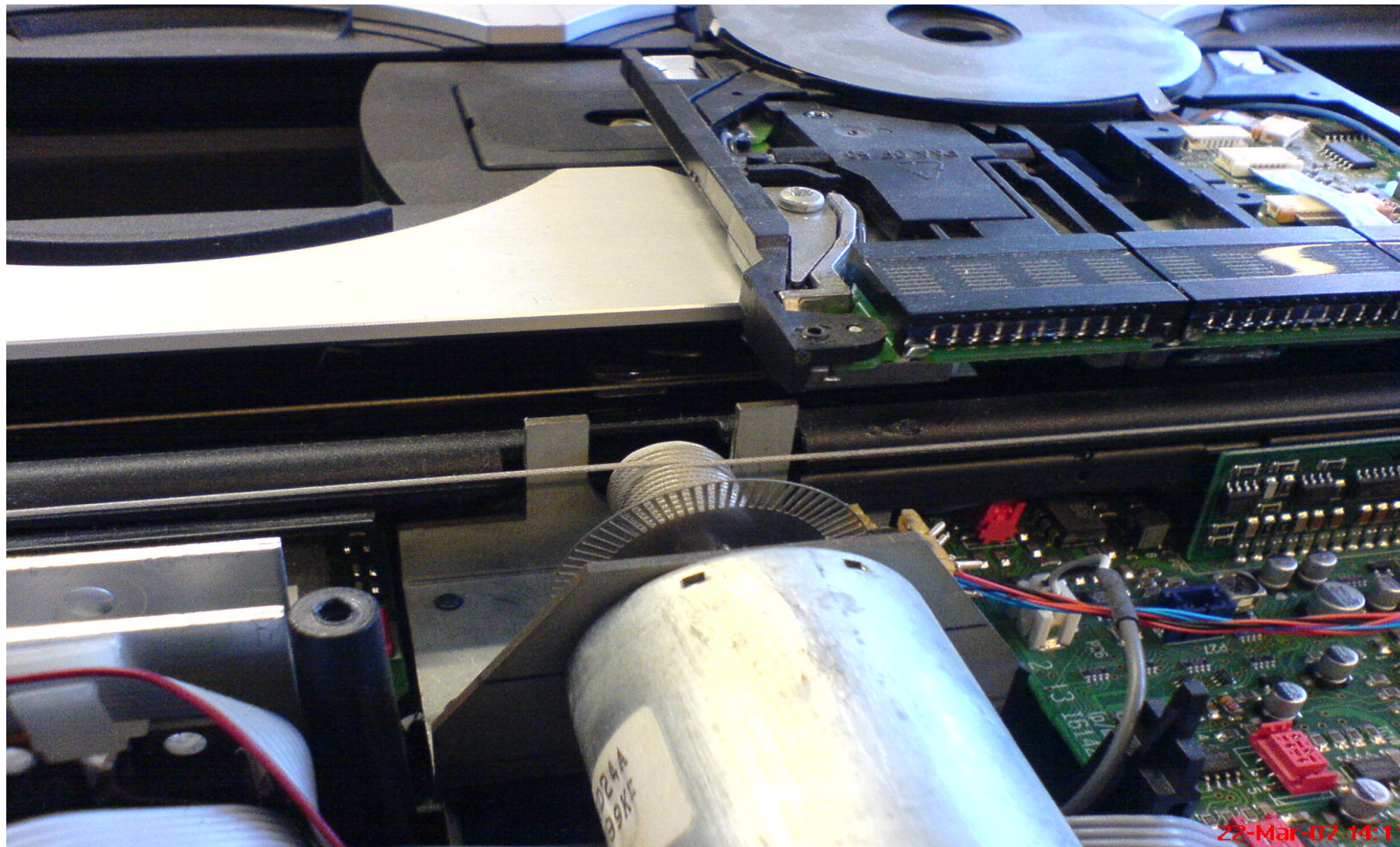


Figure 2: DC-motor and its digital encoder

Operation of the sledge system

- *Slow mode* - when the glass cover is opened, the sledge should move at a slow speed around 0.16m/s;
- *Fast mode* - when the glass cover is closed, the sledge should move at a high speed around 0.8m/s.

Speed profiles

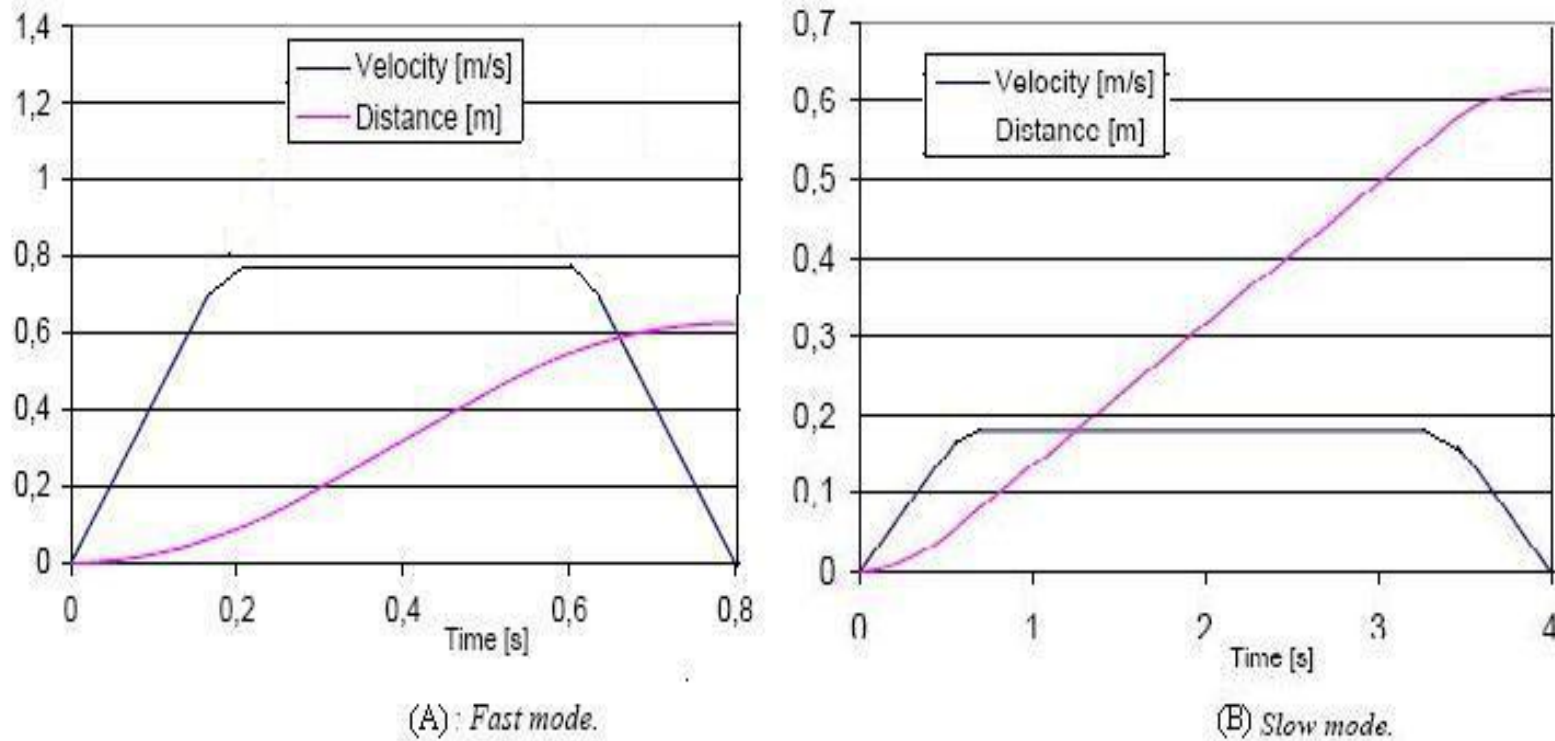


Figure 3: A set of speed profiles for control under fast and slow modes

Current problem...

- A kind of PID controller apparently is used to control the sledge system, and the controlled system performances very well with a less than 10% oscillation when the sledge moves around a constant speed
- The current PID controller doesn't cooperate with the new selected motor very well, for example, the speed oscillation becomes up to 30% when the sledge should run at a constant speed, no matter the system is under slow or fast mode.

State of the Art

There are extensive studies on the control of optical disk drives [Philips_Sony:1991]

- dual control of the sledge and voice coil motor
- coupling between focusing and tracking dynamics
- Robust control techniques such as H_∞ control

In the following, we will investigate several simple model-based control techniques for control of the BeoSound 9000 sledge system, namely, digital PID control, digital PI control with anti-windup, and an observer-based state feedback with integral control. The developed controllers are implemented into a TI MSP430F149 microprocessor.

Contents

1. Introduction
2. **Mathematical Model of the considered Sledge System**
3. Parameter Identification
4. Simulation and Model Validation
5. Control Design and Test Results
6. Conclusions

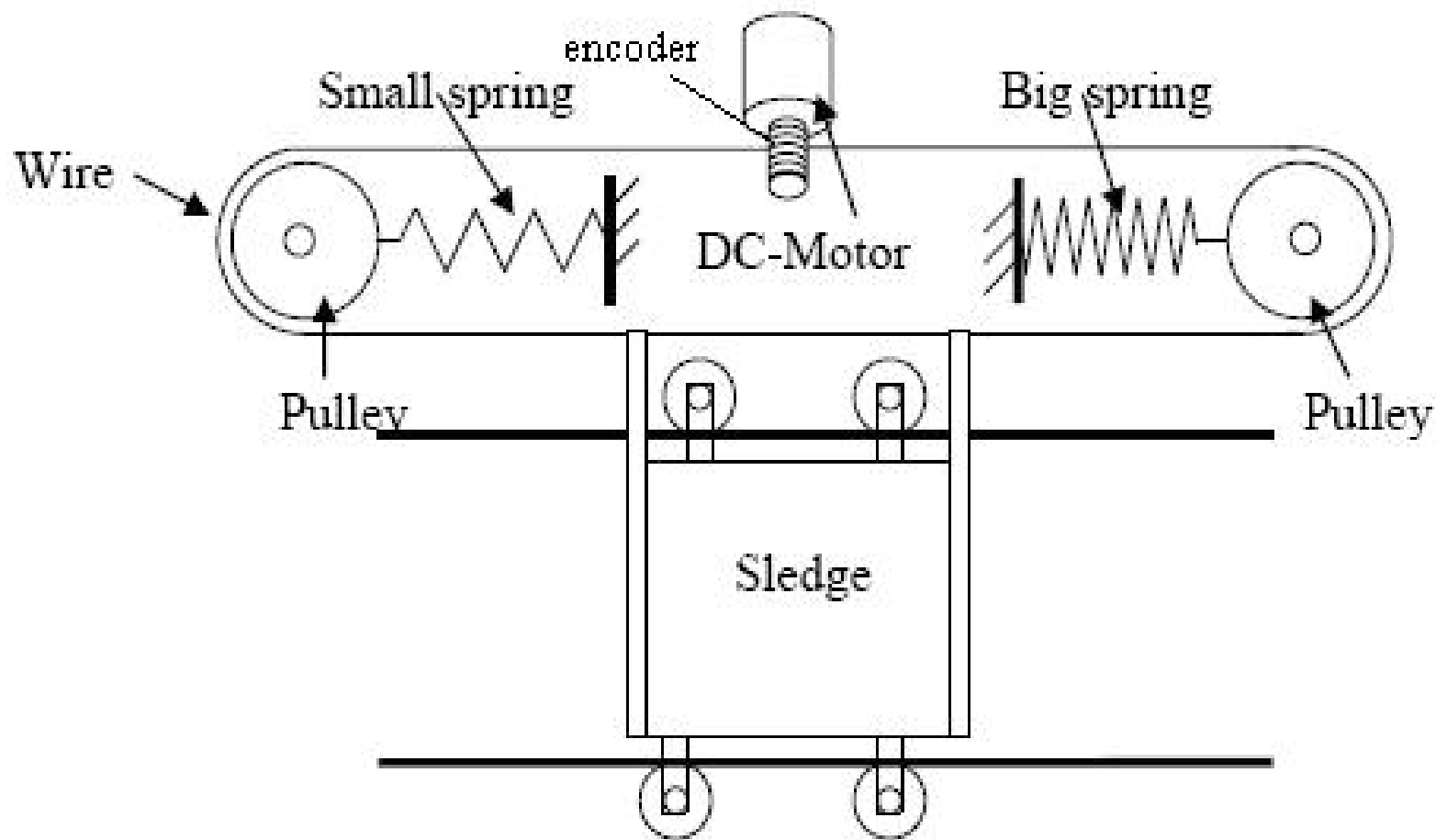


Figure 4: Schematic diagram of BeoSound 9000 sledge system

Modeling the DC-Motor (1)

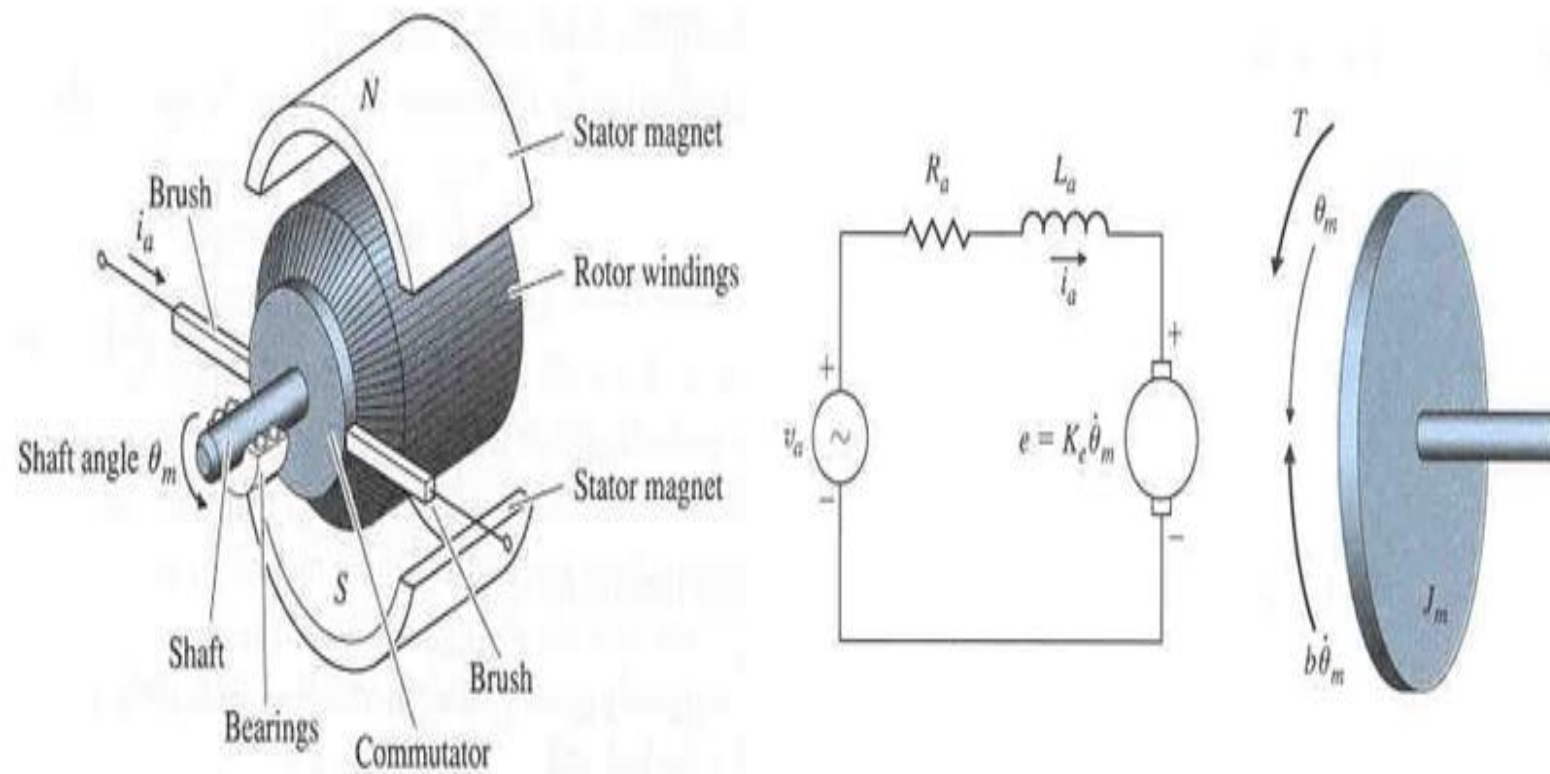


Figure 5: Schematic modeling of a DC motor

Modeling the DC-Motor (2)

The electrical part of the DC-motor is described by

$$u_a(t) = L_a \frac{di_a(t)}{dt} + R_a i_a(t) + V_{EMF}(t), \quad (1)$$

The mechanical part of the DC-motor is described by

$$T_M(t) - T_f(t) - T_e(t) = J_M \frac{d\omega_M(t)}{dt}. \quad (2)$$

(1) and (2) are linked through the following torque and EMF equations:

$$T_M(t) = K_t i_a(t), \quad V_{EMF}(t) = K_e \omega_M(t). \quad (3)$$

Modeling the Mechanical Unit (1)

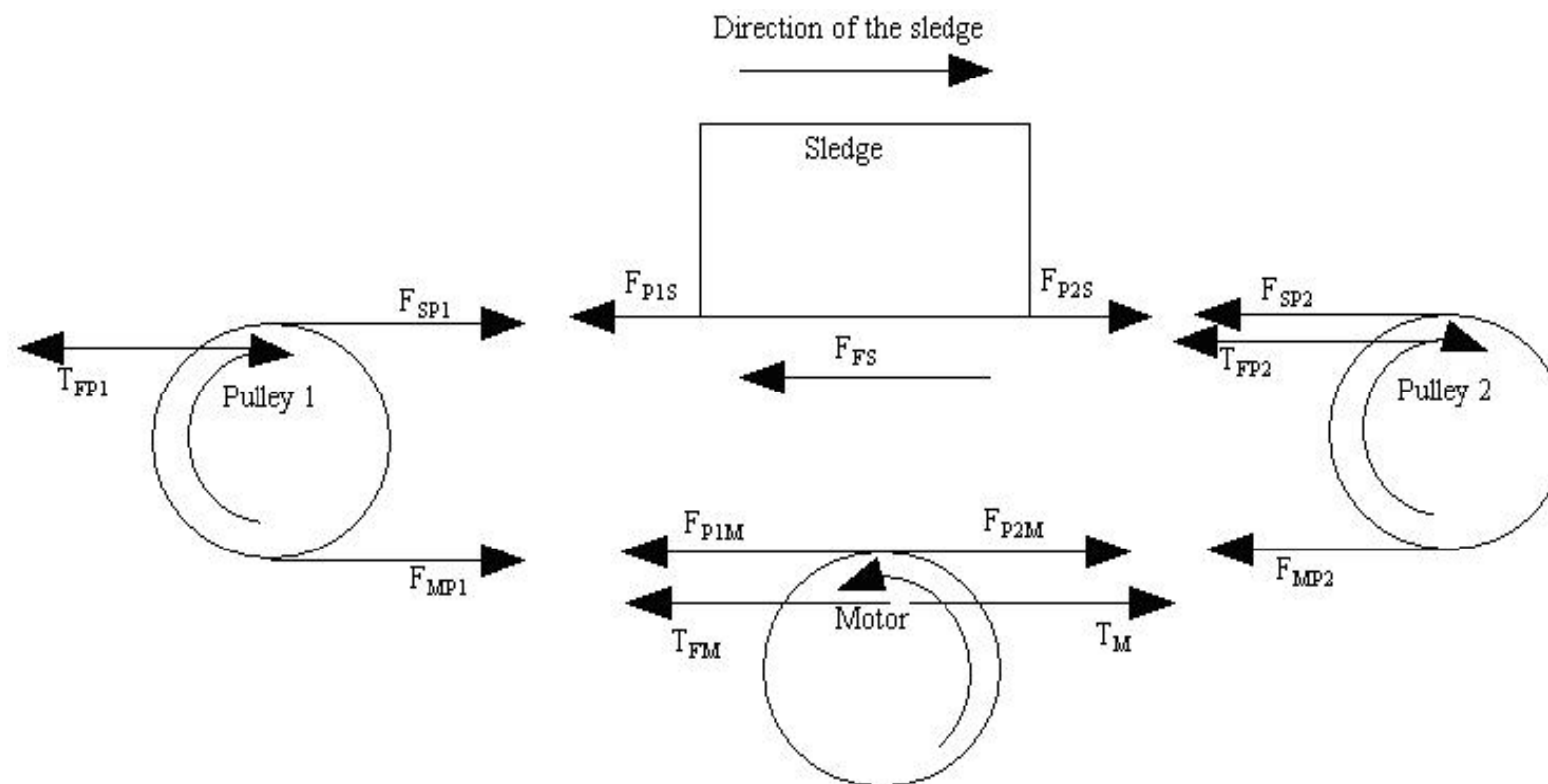


Figure 6: Free body diagram of the mechanic part

Modeling the Mechanical Unit (2)

We assume

- the connection wire is inelastic and without mass;
- the suspension springs are assumed static, i.e., the centers of the two pulleys can never move;
- the two pulleys are identical.

Modeling the Mechanical Unit (3)

The dynamics of the DC-motor part can be described as

$$J_M \frac{d^2 \theta_M(t)}{dt^2} = T_M + r_M (F_{P1M} - F_{P2M}) - T_f. \quad (4)$$

The dynamics of the two pulleys can be described as

$$\begin{cases} J_P \frac{d^2 \theta_{P1}(t)}{dt^2} = r_p (F_{SP1} - F_{MP1}) - T_{FP1}, \\ J_P \frac{d^2 \theta_{P2}(t)}{dt^2} = r_p (F_{MP2} - F_{SP2}) - T_{FP2}. \end{cases} \quad (5)$$

The dynamics of the sledge can be described as

$$M_s \frac{d^2 x(t)}{dt^2} = F_{P2S} - F_{P1S} - F_S + mgsin\Phi. \quad (6)$$

By knowing the relationships

$$\begin{aligned} |F_{SP1}| &= |F_{P1S}|, & |F_{SP2}| &= |F_{P2S}|, \\ |F_{MP1}| &= |F_{P1M}|, & |F_{MP2}| &= |F_{P2M}|, \\ r_p \frac{d^2 \theta_{P1}}{dt^2} &= \frac{d^2 x}{dt^2}, & r_p \frac{d^2 \theta_{P2}}{dt^2} &= \frac{d^2 x}{dt^2}, & r_M \frac{d^2 \theta_M}{dt^2} &= \frac{d^2 x}{dt^2}, \end{aligned} \quad (7)$$

the dynamics of the mechanical part can be described in a compact form as

$$M_t \frac{d^2 x(t)}{dt^2} = \frac{1}{r_M} T_M(t) - F_f(t), \quad (8)$$

where

$$M_t = \frac{2J_P}{r_P^2} + \frac{J_M}{r_M^2} + M_s,$$

$$F_f(t) = \frac{1}{r_P^2} (F_{FP2} + F_{FP1}) - \frac{1}{r_M^2} F_f - F_S.$$

Combining (1), (3) and (8), the model of the entire sledge system can be obtained. The block diagram of the entire system is shown in Fig.7.

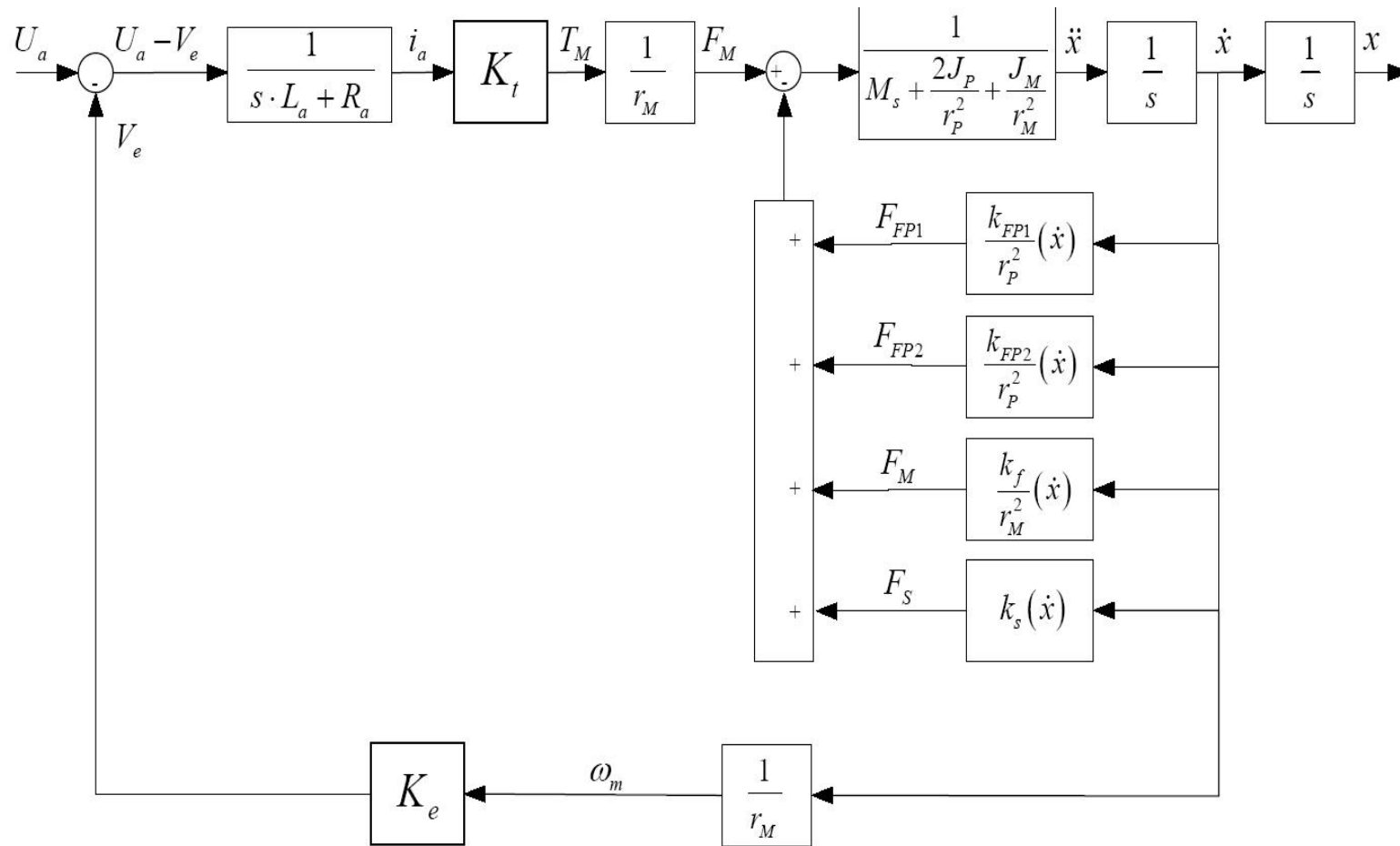


Figure 7: Block diagram of entire sledge system

Contents

1. Introduction
2. Mathematical Model of the considered Sledge System
3. **Parameter Identification**
4. Simulation and Model Validation
5. Control Design and Test Results
6. Conclusions

Identification of Motor Parameters

- The armature coil resistance can be directly measured, which is $R_a = 11.1\Omega$
- In order to identify the motor constant K_t (EMF constant $K_e = K_t$), the considered motor is driven by another motor at a constant speed. Meanwhile, the angular velocity of the considered motor is measured by the digital encoder along with voltage over the armature terminals. The system coefficient K_e is then estimated as $K_e = K_t = 5.9e - 2$
- The armature inductance $L_a = 9.688mH$ is estimated through the time constant of a simple circuit as shown in Fig.8 where the output is the measured voltage over a serial connected resistor.

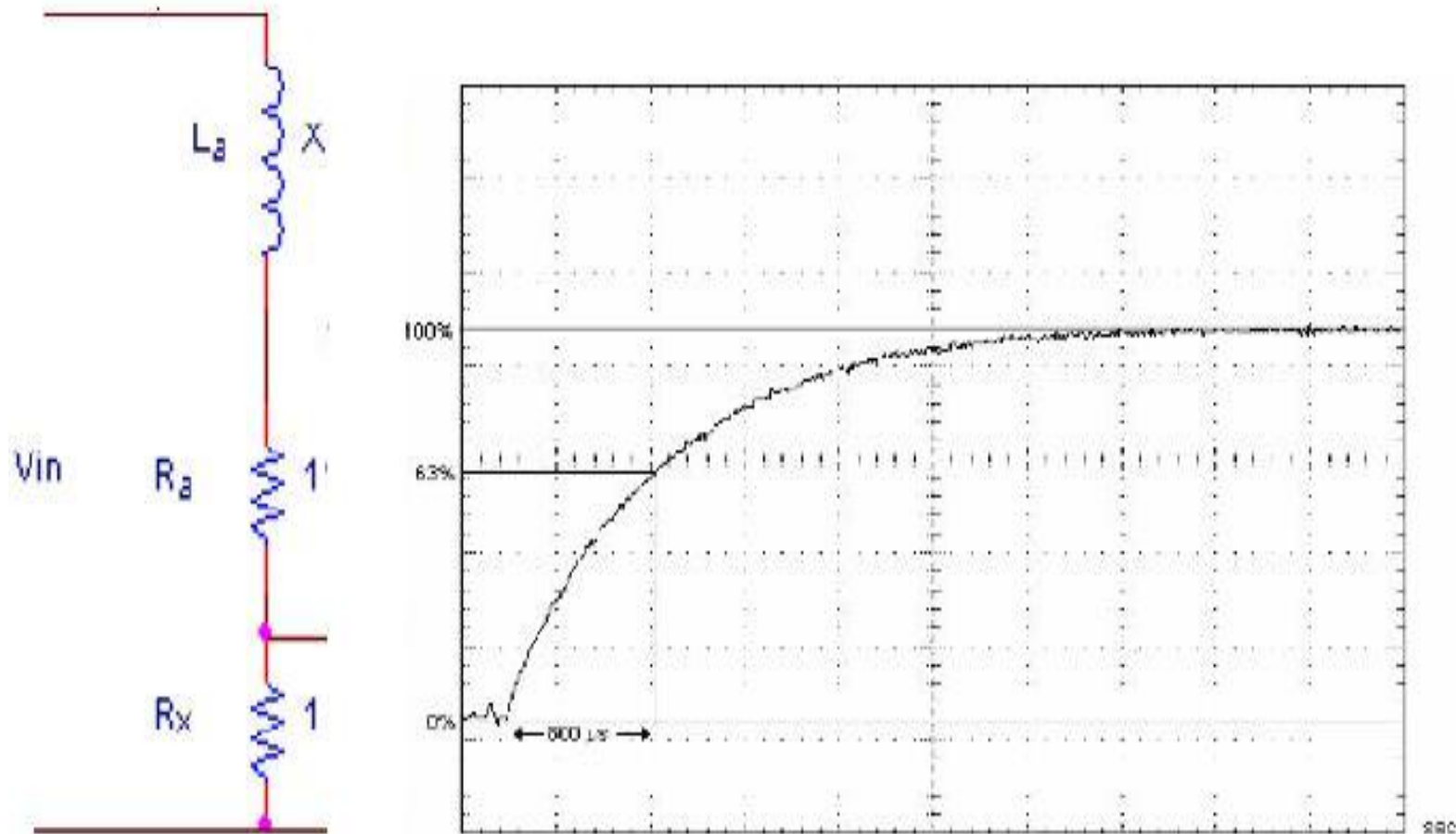


Figure 8: Estimation of armature inductance

Identification of Mechanical Part - total mass

Basic idea: Use the relationship between the input voltage to the motor and the sledge speed (first-order system), the total mass can be derived from the estimated time constant.

Procedure:

- Simplification of motor dynamic: Due to its small value, the inductance of the used DC-motor can be neglected from (1). The torque generated by the DC-motor can then be estimated by

$$T_M(t) = \frac{K_t}{R_a} \left(u_a - K_e \frac{\dot{x}(t)}{r_M} \right), \quad (9)$$

where $\dot{x}(t)$ denotes the speed of the sledge. Then (8) can be simplified as

$$M_t r_M \frac{d^2 x(t)}{dt^2} = \frac{K_t}{R_a} \left(u_a - K_e \frac{\dot{x}(t)}{r_M} \right) - r_M F_f(t).$$

- Assumption of frictions: We assume the force due to friction $F_f(t)$ is

linearly dependent on the speed, i.e.,

$$F_f(t) = K_f \dot{x}(t).$$

The analysis of this assumption is discussed in the following subsection.

- Considered transfer function: Then the transfer function from the input voltage $u_a(t)$ ($U_a(s)$) to the sledge speed $\dot{x}(t)$ ($\dot{X}(s)$) is

$$\frac{\dot{X}(s)}{U_a(s)} = \frac{K_t r_M}{M_t r_M^2 R_a s + (K_t K_e + r_M K_f)}, \quad (10)$$

- The system time constant is

$$\tau \hat{=} \frac{M_t r_M^2 R_a}{K_t K_e + r_M K_f}. \quad (11)$$

It is observed that M_t is only relevant to the time constant of the system (10). However, so far the system parameter K_f is unknown. Therefore, an experiment is arranged to identify M_t without influence of K_f

- **Designed experiment:** drive the sledge system with a constant voltage input and measure the speed through the digital encoder. This experiment is done under different situations for which the masses of the sledge unit are different by adding extra known masses on top of the sledge unit. The time constants for different load situations can be determined based on experimental data as shown in Fig.9.

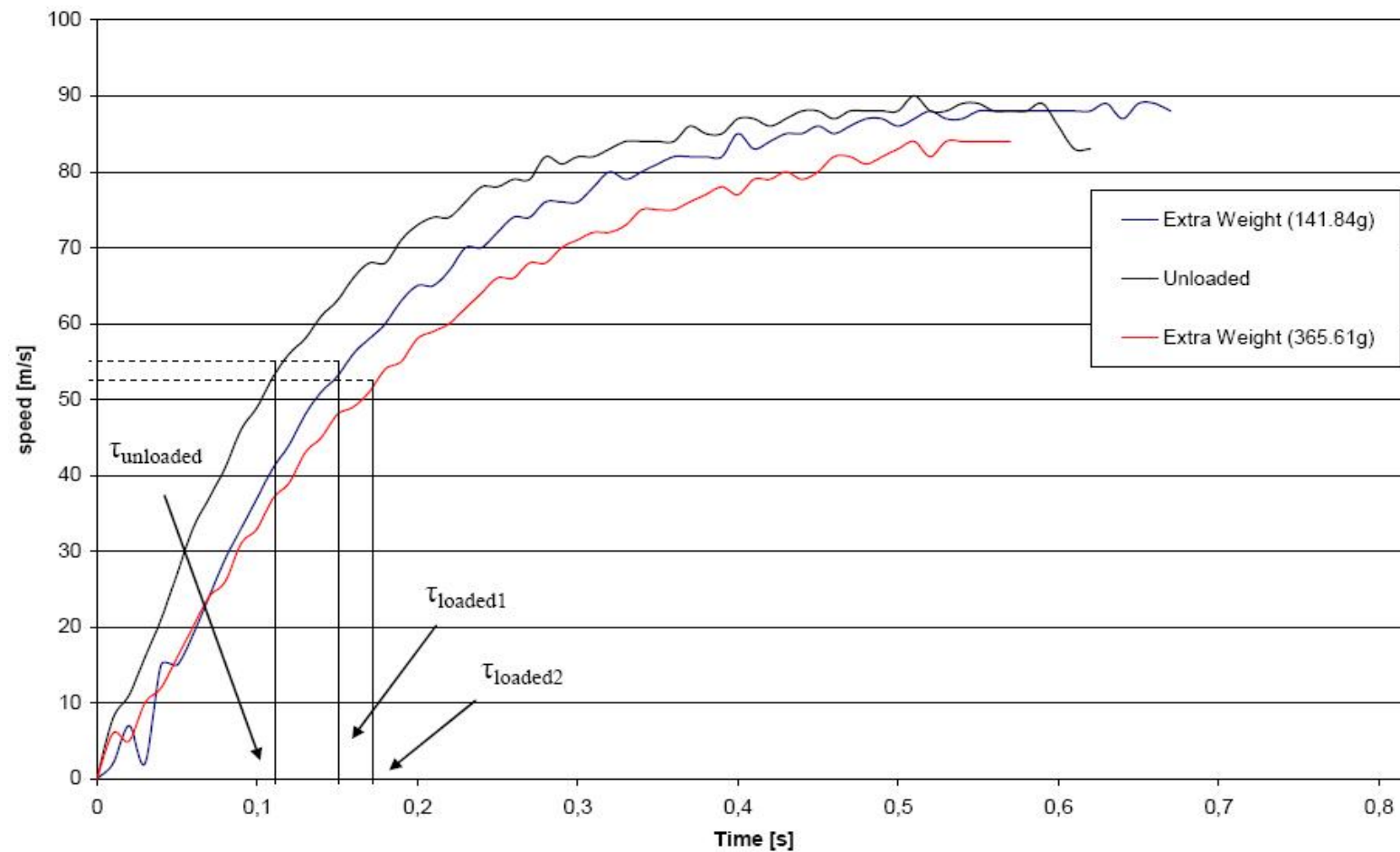


Figure 9: Estimation of total mass using step responses

- Estimation of total mass: the time constant of a testing system with

known load m_{ex} is

$$\tau_{ex} = \frac{(M_t + m_{ex})r_M^2 R_a}{K_t K_e + r_M K_f}. \quad (12)$$

$$\tau \hat{=} \frac{M_t r_M^2 R_a}{K_t K_e + r_M K_f}. \quad (13)$$

By combining (13) and (12), the mass M_t can be determined by

$$M_t = m_{ex} \frac{\tau}{\tau_{ex} - \tau}. \quad (14)$$

An average of results from several tests is used as the value of the system, it is $M_t = 0.57kg$.

Friction Analysis

There are two types of friction for mechanical movement that needs to be identified:

- static friction: the stick force that the system needs to overcome in order to start moving.

The static friction is estimated by using a Newton meter, and it is $F_{static} = 4.6N$.

- dynamic friction consists of viscous friction which is speed dependent and coulomb friction which is a dry force

Viscous Friction

Basic idea: experimentally estimate the friction force via speed curve...

Procedure (1): Use the free response analysis. The maximum input 14v is applied to the DC-motor until the sledge system reaches a constant speed. Then power is switched immediately, meanwhile the sledge speed is recorded until the sledge stop. During the free response period, there are only friction forces (viscous and coulomb frictions) acting on the sledge system. By estimating the deceleration at several selected speed points for the free response period and using the total mass M_t estimated before, then a figure showing the relationship between the friction forces via speed is presented in Fig.10 (right figure). The viscous coefficient thereby can be estimated.

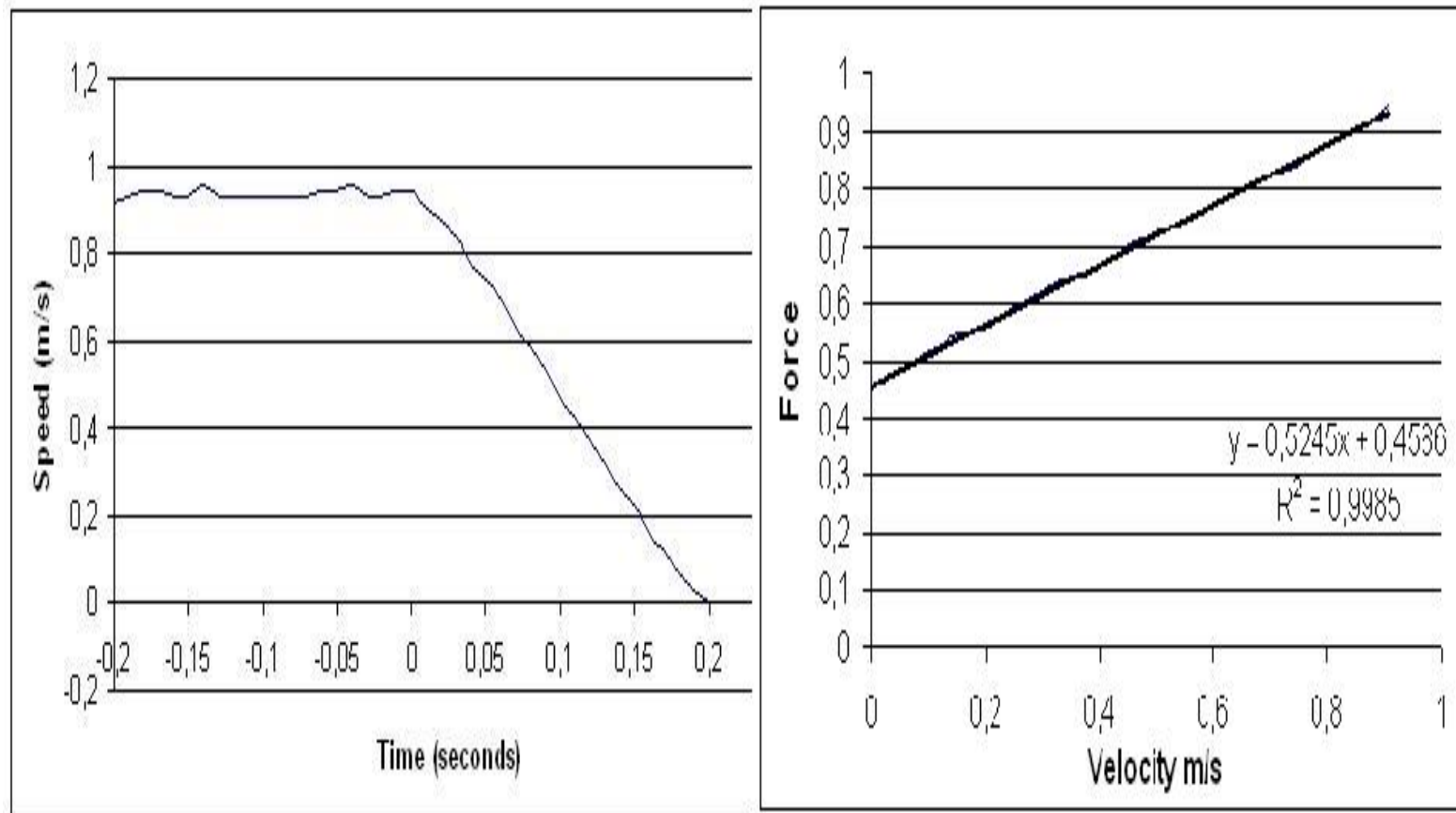


Figure 10: Measured speed of an inverse step response and the estimated viscous friction force

Procedure (2): use the relationships at the steady-state situations:

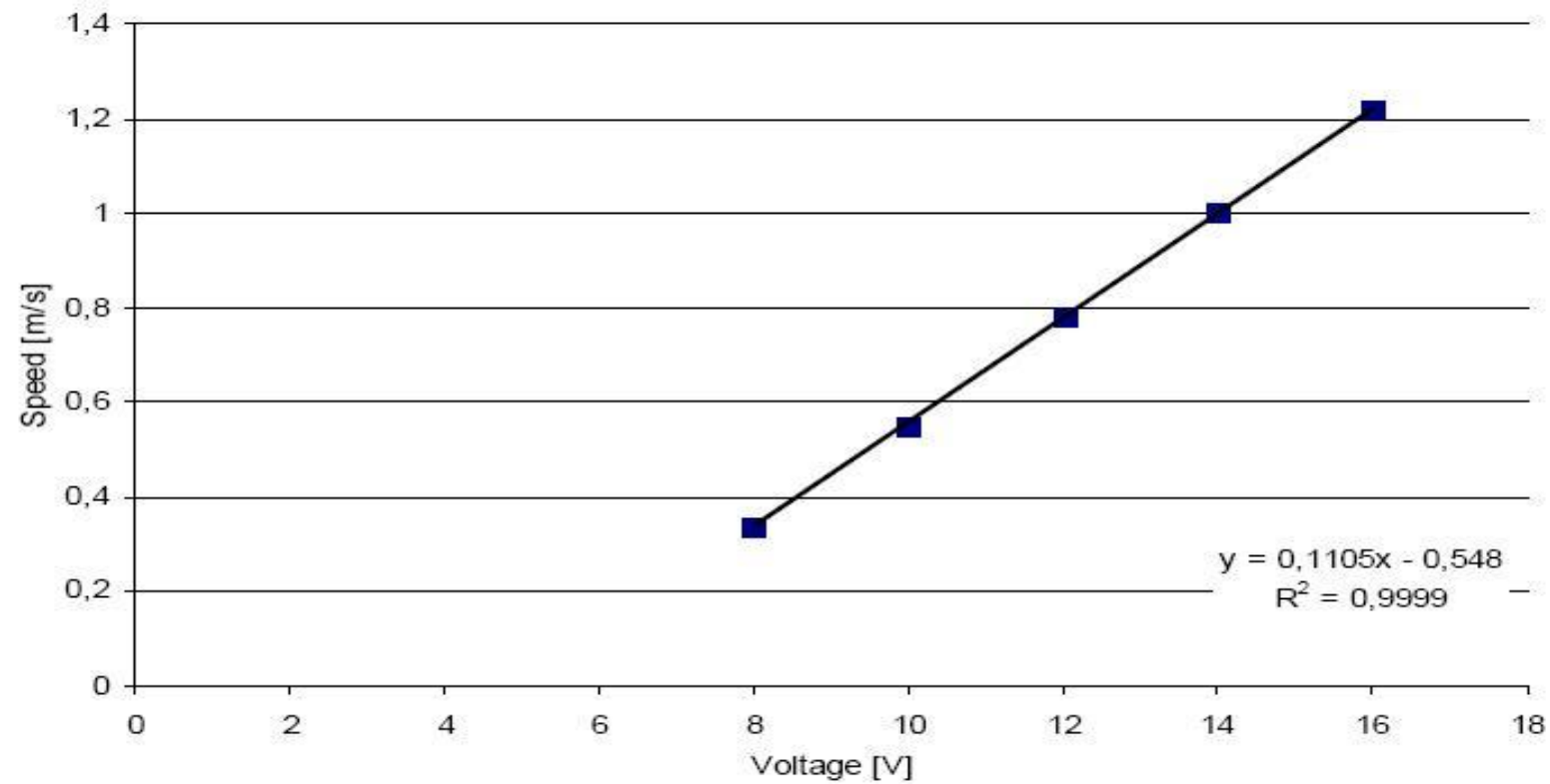


Figure 11: Measured steady-state speeds and corresponding inputs

Coulomb Friction

The coulomb friction is always present during the movement. Once the viscous friction coefficient has been identified, the coulomb friction can be estimated using the measurement when the sledge moves at a constant speed. The basic idea is: When the sledge moves at a constant speed which can be measured through the encoder, there is the force balance, i.e.,

$$F_M = k_{viscous}\dot{x} + F_{coulomb}, \quad (15)$$

where F_M is the force generated by the DC-motor acting on the wire. F_M can be estimated through $F_M = \frac{T_M}{r_M} = \frac{K_t i_a}{r_M}$ if the armature current i_a can be measured. Then, using the measured sledge speed \dot{x} and the viscous coefficient estimated in last subsection, the coulomb friction can be estimated as $F_{coulomb} = F_M - k_{viscous}\dot{x}$. For our case, there is $F_{coulomb} = 2.98N$.

Total friction estimation

The total friction part is estimated as

$$F_f(\dot{x}) = \begin{cases} 1.25\dot{x}(t) + 2.98, & \dot{x}(t) \succeq 0 \\ 1.25\dot{x}(t) - 2.98, & \dot{x}(t) \preceq 0 \\ 4.6 & \dot{x}(t) = 0 \end{cases} \quad (16)$$

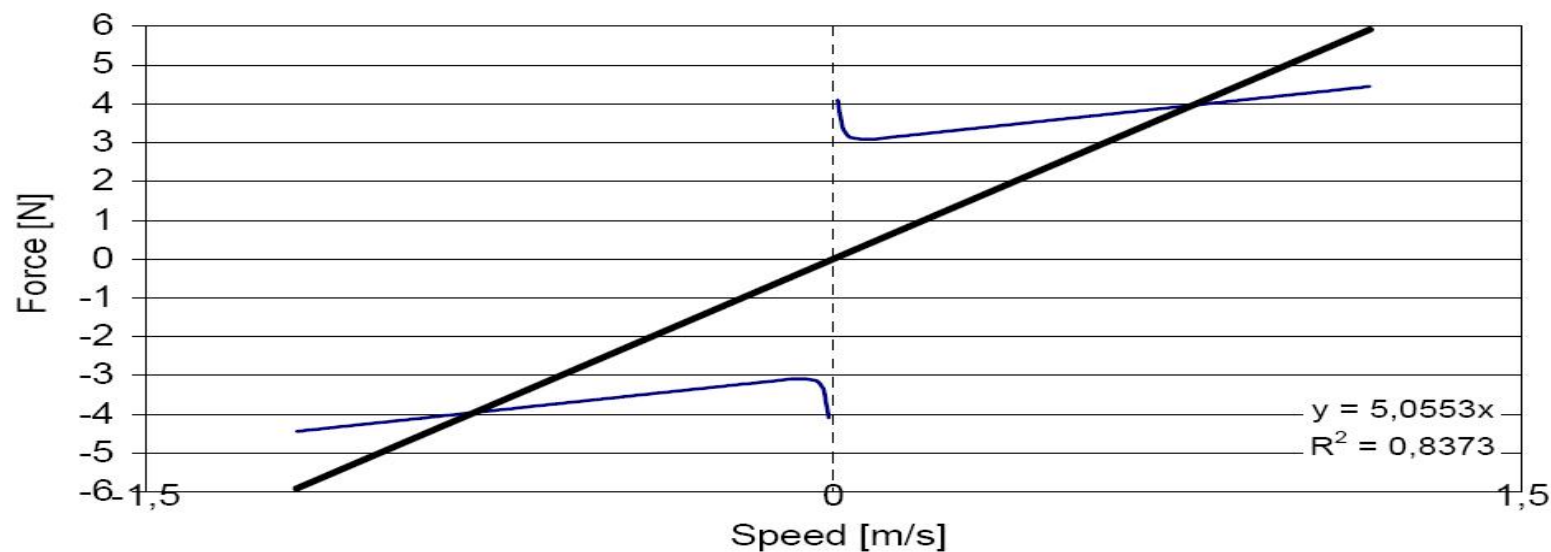
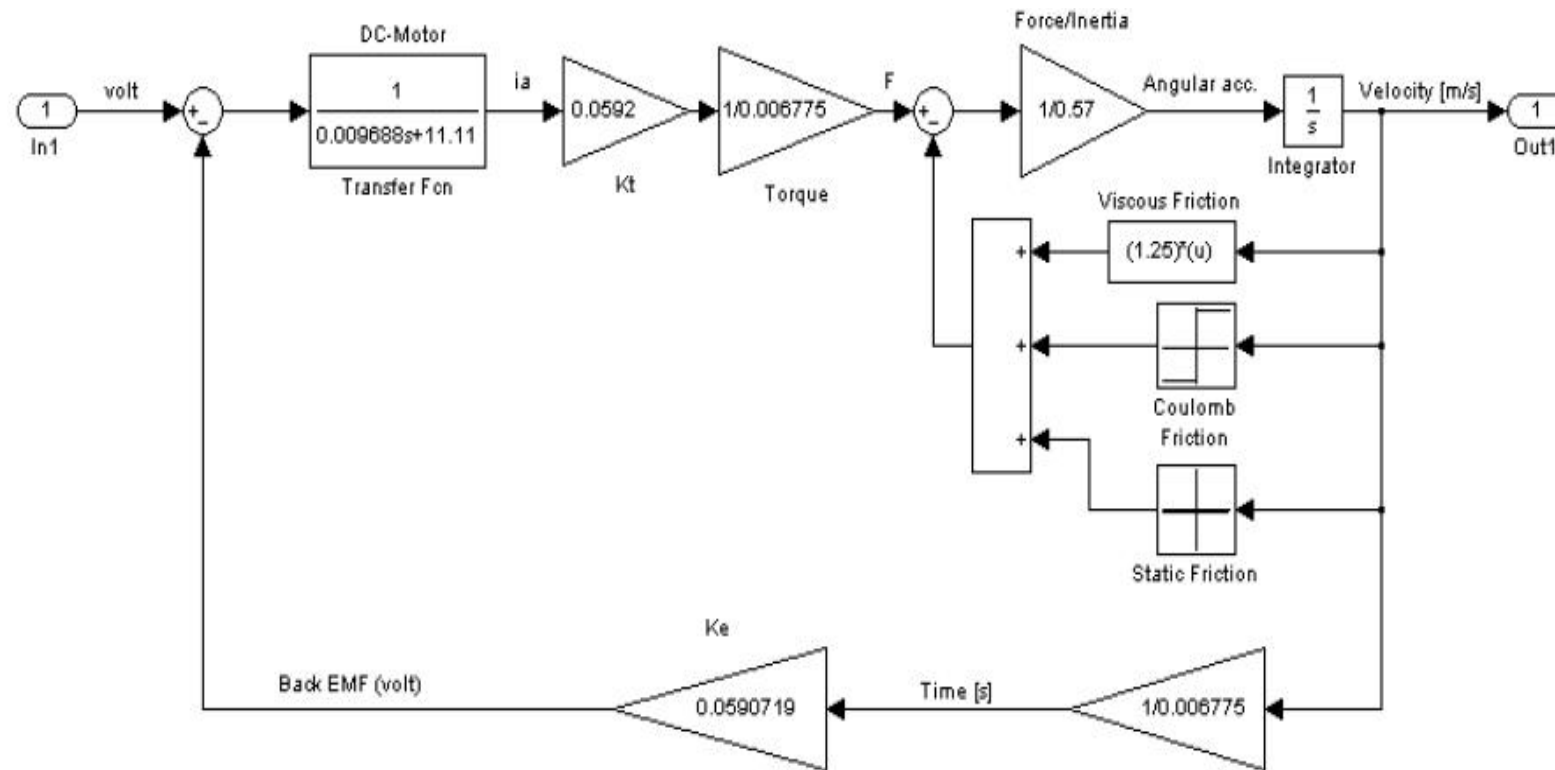


Figure 12: Friction curve of the entire sledge system

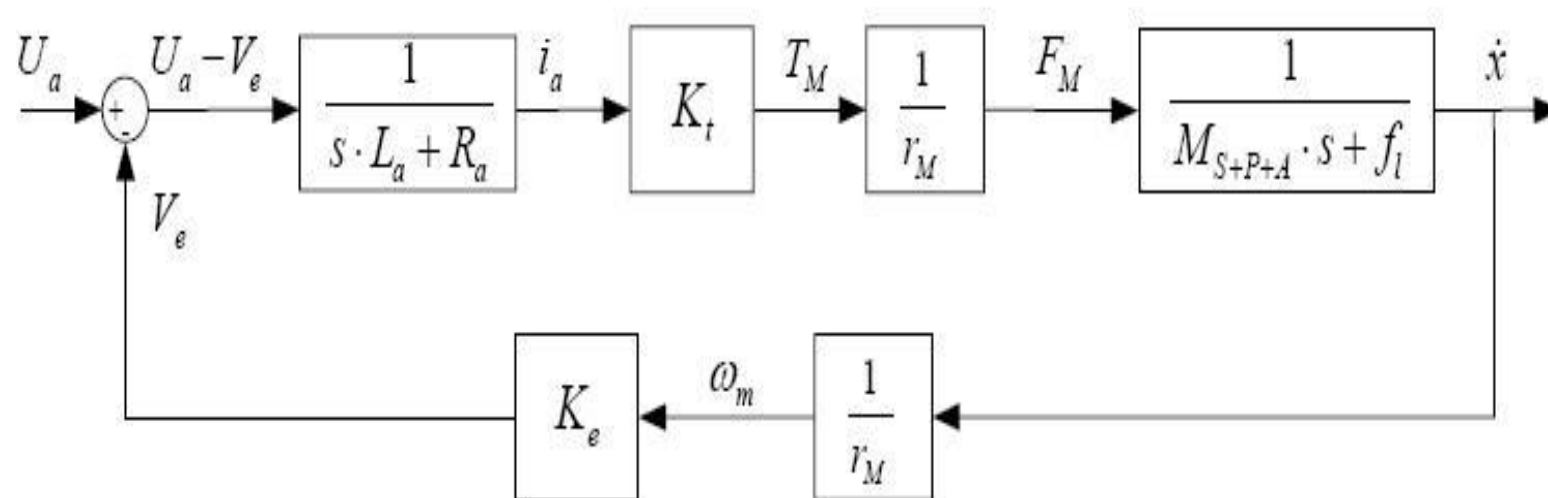
Contents

1. Introduction
2. Mathematical Model of the considered Sledge System
3. Parameter Identification
4. **Simulation and Model Validation**
5. Control Design and Test Results
6. Conclusions

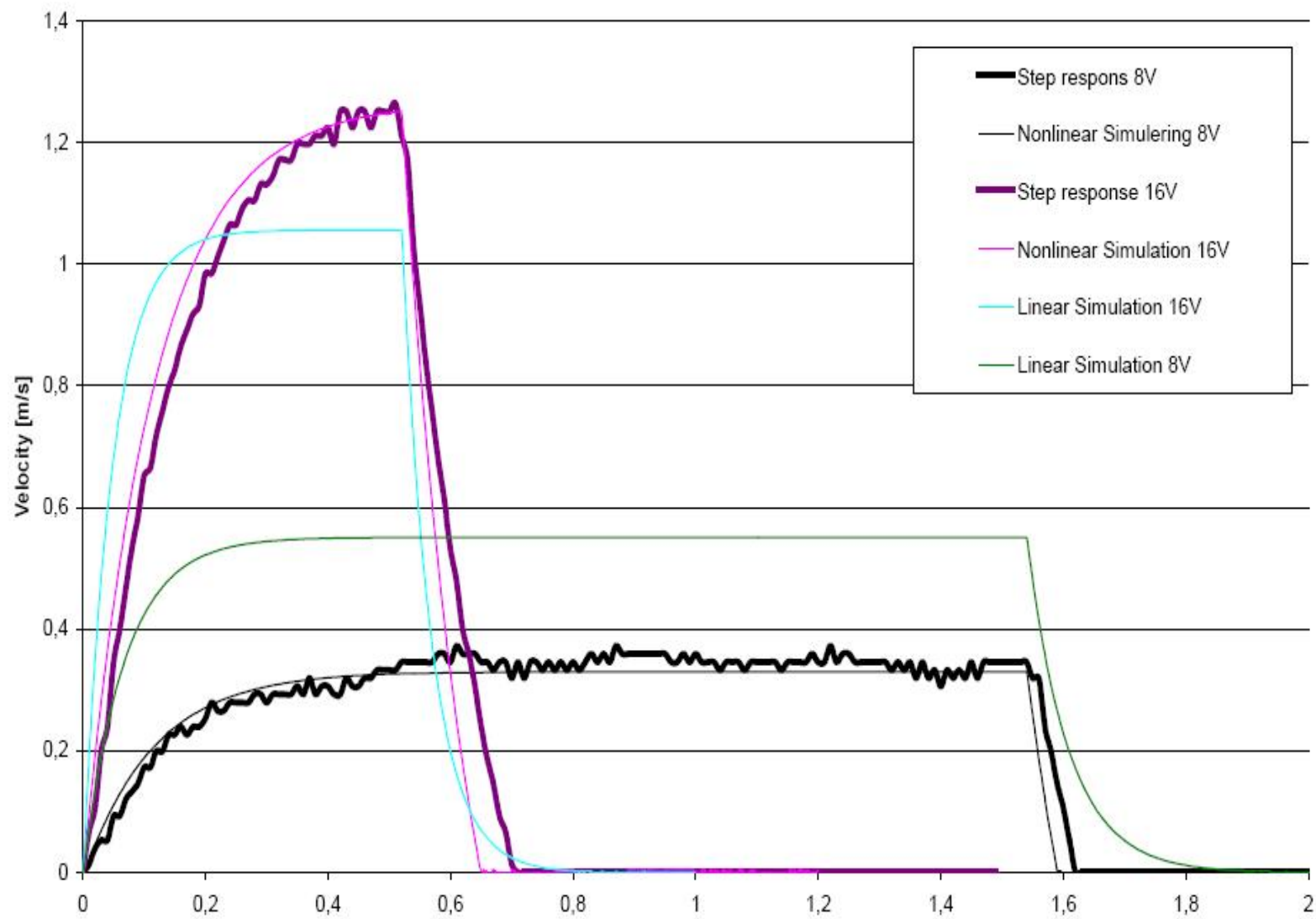
Simulation model - Nonlinear model



Simulation model - linear model



Model validation



Contents

1. Introduction
2. Mathematical Model of the considered Sledge System
3. Parameter Identification
4. Simulation and Model Validation
5. **Control Design and Test Results**
6. Conclusions

Control Objectives

The following demands are proposed by Bang & Olufsen A/S regarding the dynamic performance of the sledge system.

- *Traveling time:* The sledge unit should move from position 1 to position 6 within 0.8 (4) second for the fast-speed (slow-speed) mode;
- The oscillation of the speed during the movement should be controlled around 10%;
- The sledge should slow down below 0.3m/s at its destination for the clamps to be activated.

Control Strategies (1)

Several control methods are employed for the sledge speed control design, namely

- Standard PID controller. The Ziegler-Nichols quarter decay ratio and ultimate sensitivity methods are used to determine PID coefficients, respectively. A digital implementation is

$$u(k) = u(k-1) + K_P \left[\left(1 + \frac{T_s}{T_I} + \frac{T_D}{T_s}\right) e(k) - \left(1 + \frac{2T_D}{T_s}\right) e(k-1) + \frac{T_D}{T_s} e(k-2) \right]$$

where the sampling period T_s is 0.004 second for our case.

Control Strategies (2)

- PI controller with anti-windup. In order to explicitly control overshoot, the root locus method is used for further tuning of the P part of a developed PI controller based on the linearized model. Meanwhile, the anti-windup technique is also employed to handle the saturation problem of the DC-motor. An implementation is

If $u_{min} < u_c < u_{max}$, then

$$u(k) = u(k-1) + K_P \left[\left(1 + \frac{T_s}{T_I}\right) e(k) - e(k-1) \right];$$

If $u_c > u_{max}$ or $u_c < u_{min}$, then

$$u(k+1) = \left[1 - \frac{T_s K_a}{(1+K_a)T_I} \right] u(k) + \frac{K_P}{1+K_a} \left(1 + \frac{T_s}{T_I}\right) e(k) - \frac{K_P}{1+K_a} e(k-1) \quad (17)$$

where K_a is the slope coefficient of the anti-windup figure, which can be obtained through trial and error. u_{min} and u_{max} are the lower and upper boundary of the input signal to the DC-motor.

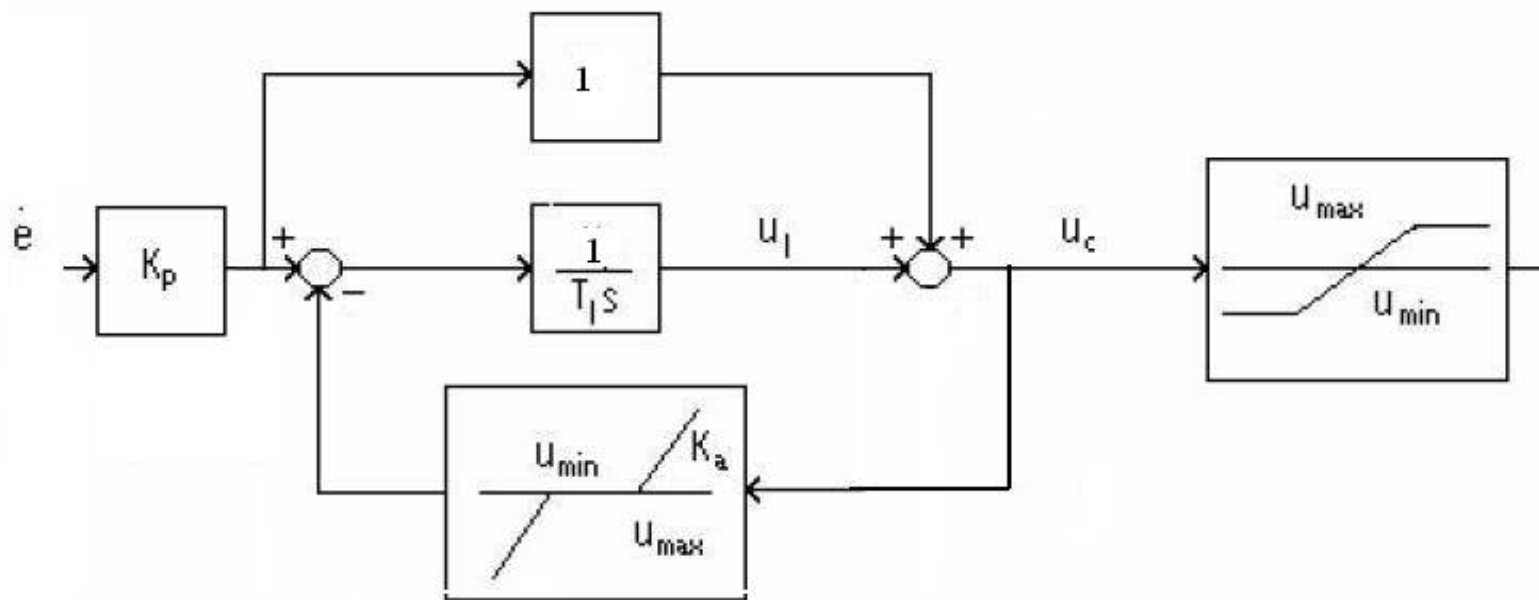


Figure 13: Structure of PI controller with anti-windup

Control Strategies (3)

- Observer-based state feedback with integral control. It is checked that the system (??) is observable and controllable. A full-order observer is designed so as to estimate the armature current i_a based on the measured \dot{x} . The observer gain is selected such that the observer is 10 times faster than the controlled system. The feedback gain and the integral gain can be combined into an augmented state space model, so that the pole placement design method is used to obtain these gains.

Results and Discussion

(1) From the test results, where $K_P = 1.9e + 2$, $K_I = 1.0e - 3$ and $K_D = 2.5e - 4$, it is observed that the sledge controlled by a PID controller developed by the Ziegler-Nichols quarter decay ratio method took a little bit over 4 sec to reach position 6 from the starting position 1 for the slow mode. There is no problem for the clamps to stop the sledge unit for the slow mode. However, the oscillation for most at the traveling period is about 25% for both slow and fast modes, which is not acceptable by the company. Similar results are also obtained for the fast mode study, where this oscillation also remains to be a problem for the fast mode

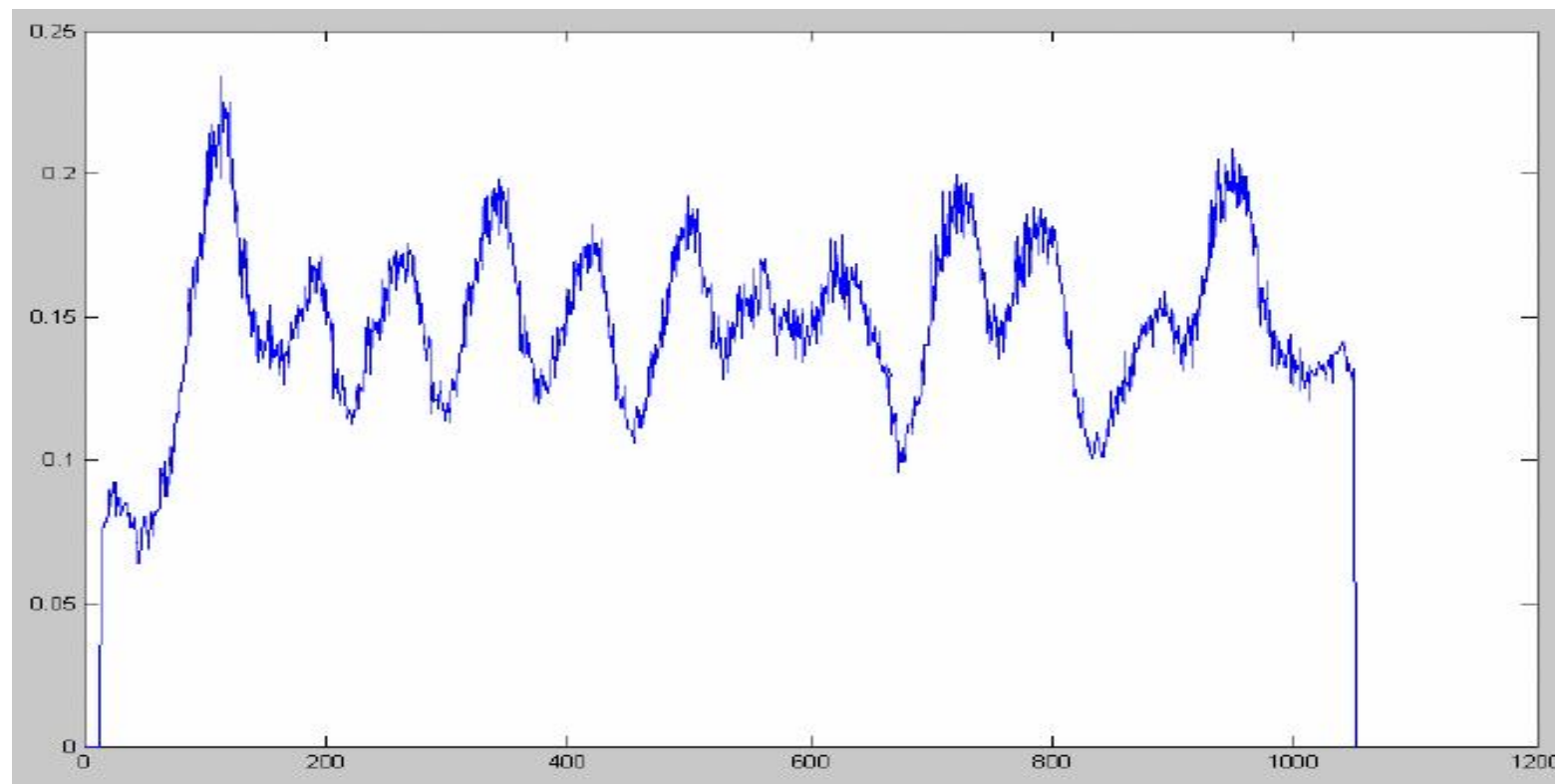


Figure 14: Result using Ziegler-Nichols quarter decay ratio method for slow mode (X-axis is samples with sampling frequency 250 Hz)

(2) In order to handle the big oscillations, the anti-windup technique is combined with a PI controller, where $K_P = 2.09$ and $K_I = 2.43e - 1$. The test result for the slow mode is shown in Fig.15. It is noticed that the system performance satisfies all requirements. A comparison of this design with a feed-forward controller where the input voltage to the DC-motor is 6.5V is shown in Fig.16. It can be observed that the controller is able to overcome the irregularities caused by irregular friction.

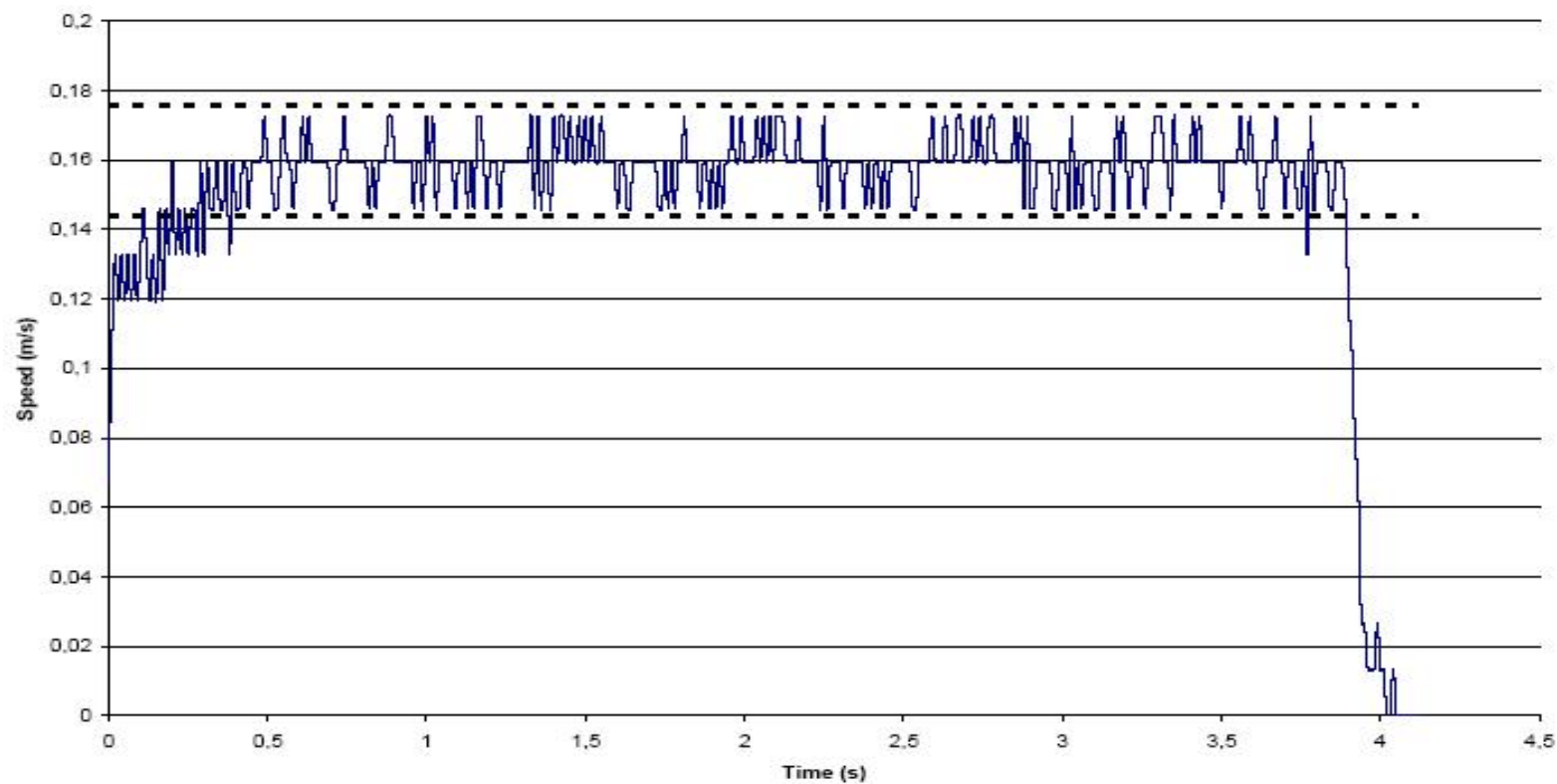


Figure 15: Speed measurement for the slow mode using PI with anti-windup

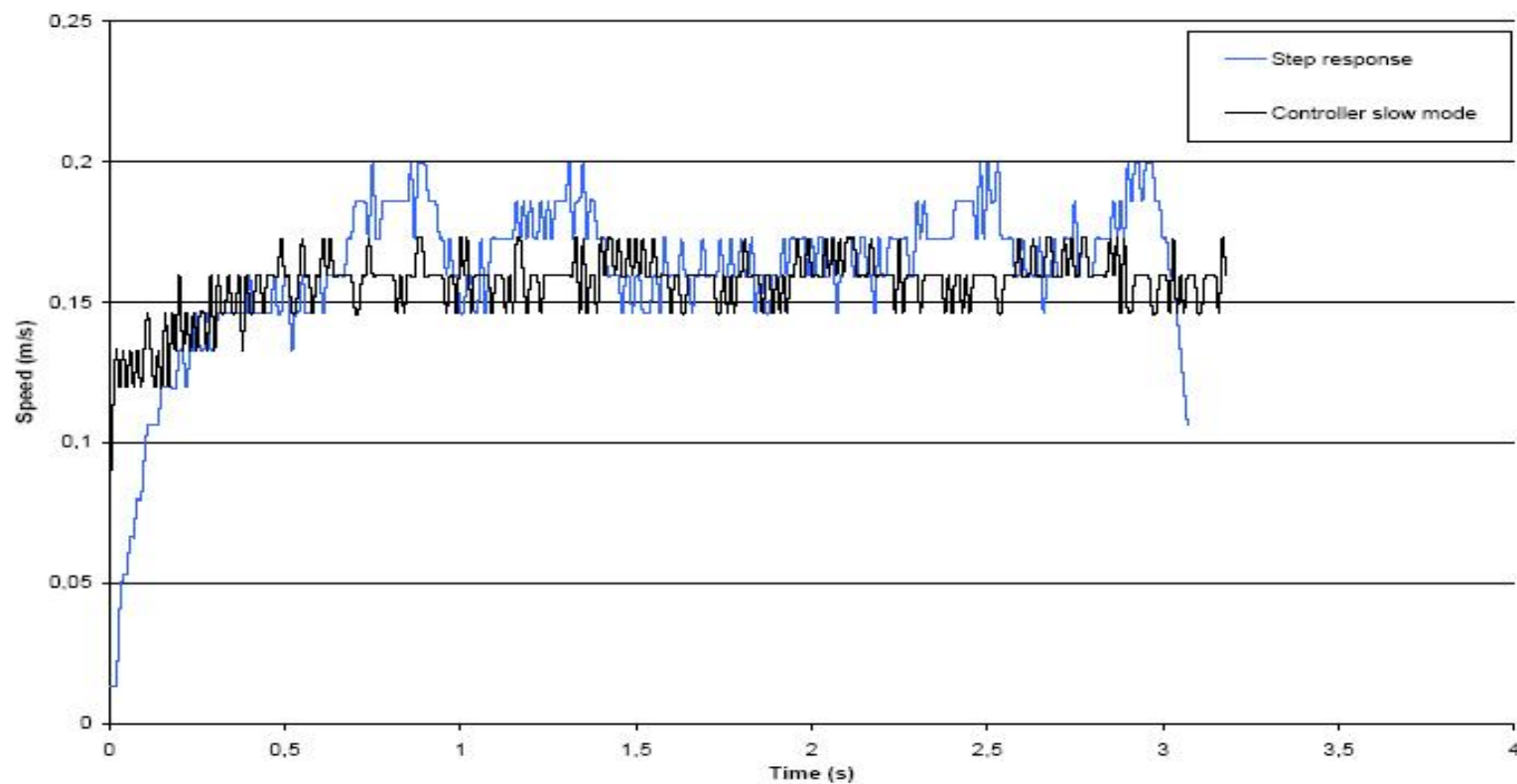
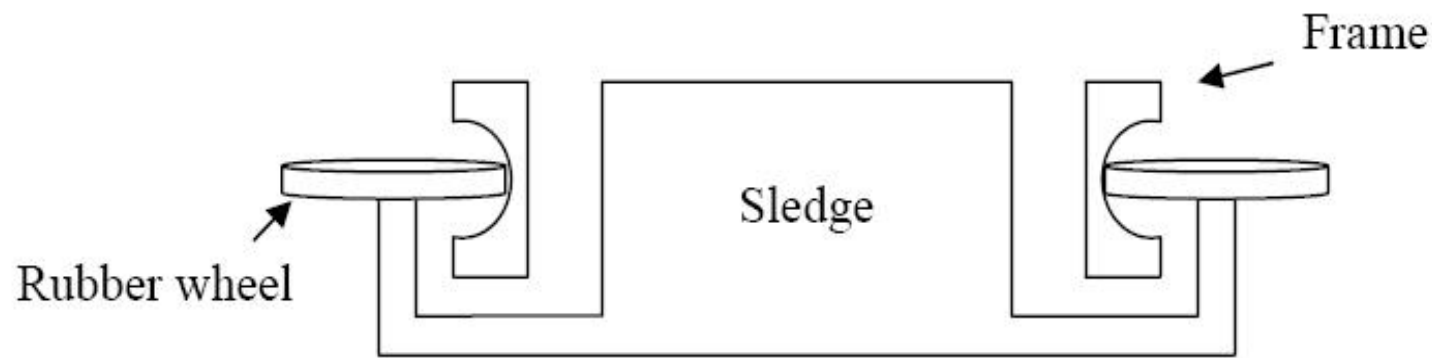
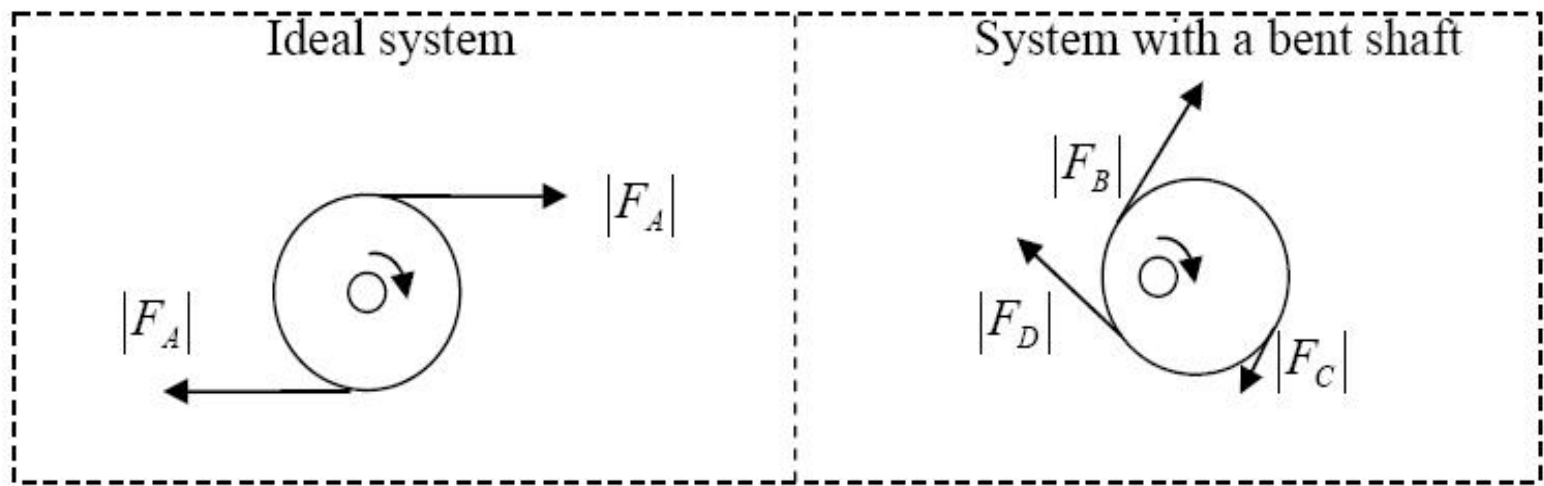


Figure 16: Performance comparison of PI (with anti-windup) with a feed-forward controller $u_a = 6.5V$



The test result for the fast mode is shown in Fig.17. It is noticed that the system performance satisfies all requirements. The comparison of this design with a feed-forward controller where the input voltage to the DC-motor is 12V shows that the controlled system has a faster response than the open-loop system, such that the traveling time is successfully limited within 0.8 seconds.

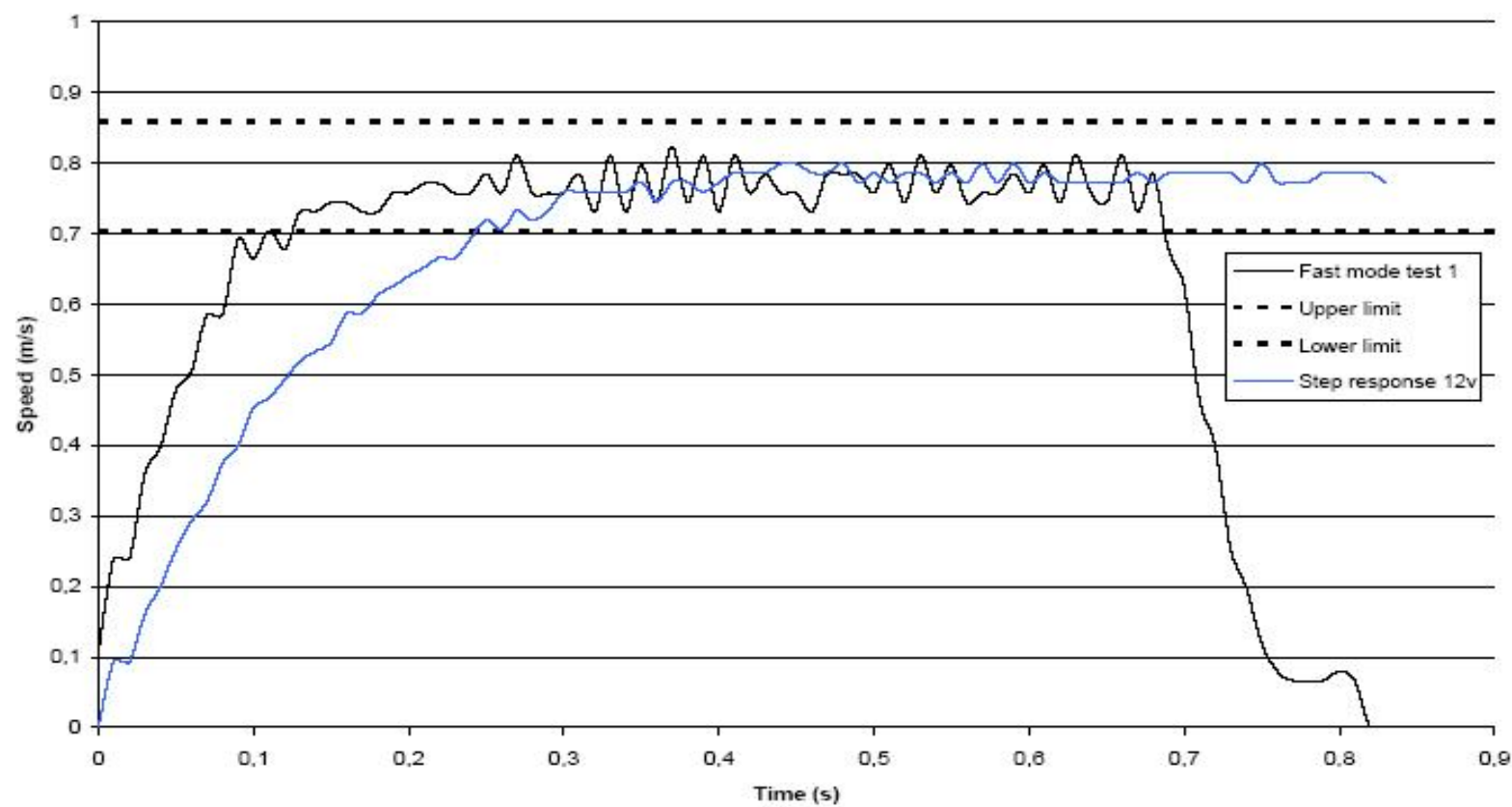


Figure 17: Speed measurements for the controlled fast mode and comparison with open-loop controller $u_a = 12V$

(3) The test results using the observer-based state feedback control with integral control for the slow and fast modes are shown in Fig.18 and Fig.19, respectively. It can be noticed that both situations are satisfied except that there are a few peaks in the slow mode over the 10% threshold, which we suspect is caused by irregular frictions due to wear out.

Comparing system performances using the PI control with anti-windup and the state space method, it can be observed that the state space method leads to a faster system than the PI control does for both slow and fast modes.

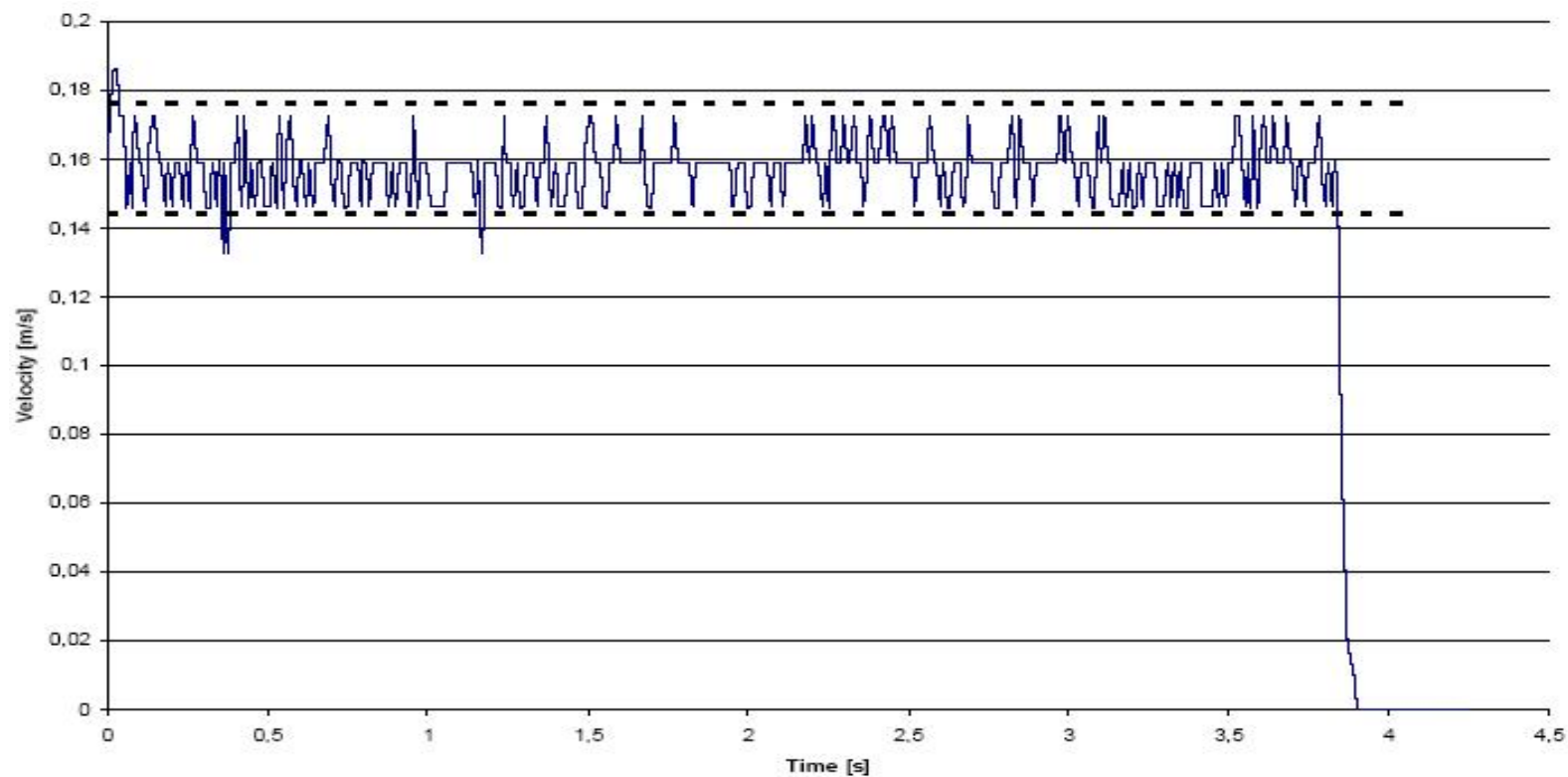


Figure 18: Speed measurement for the slow mode using state space controller

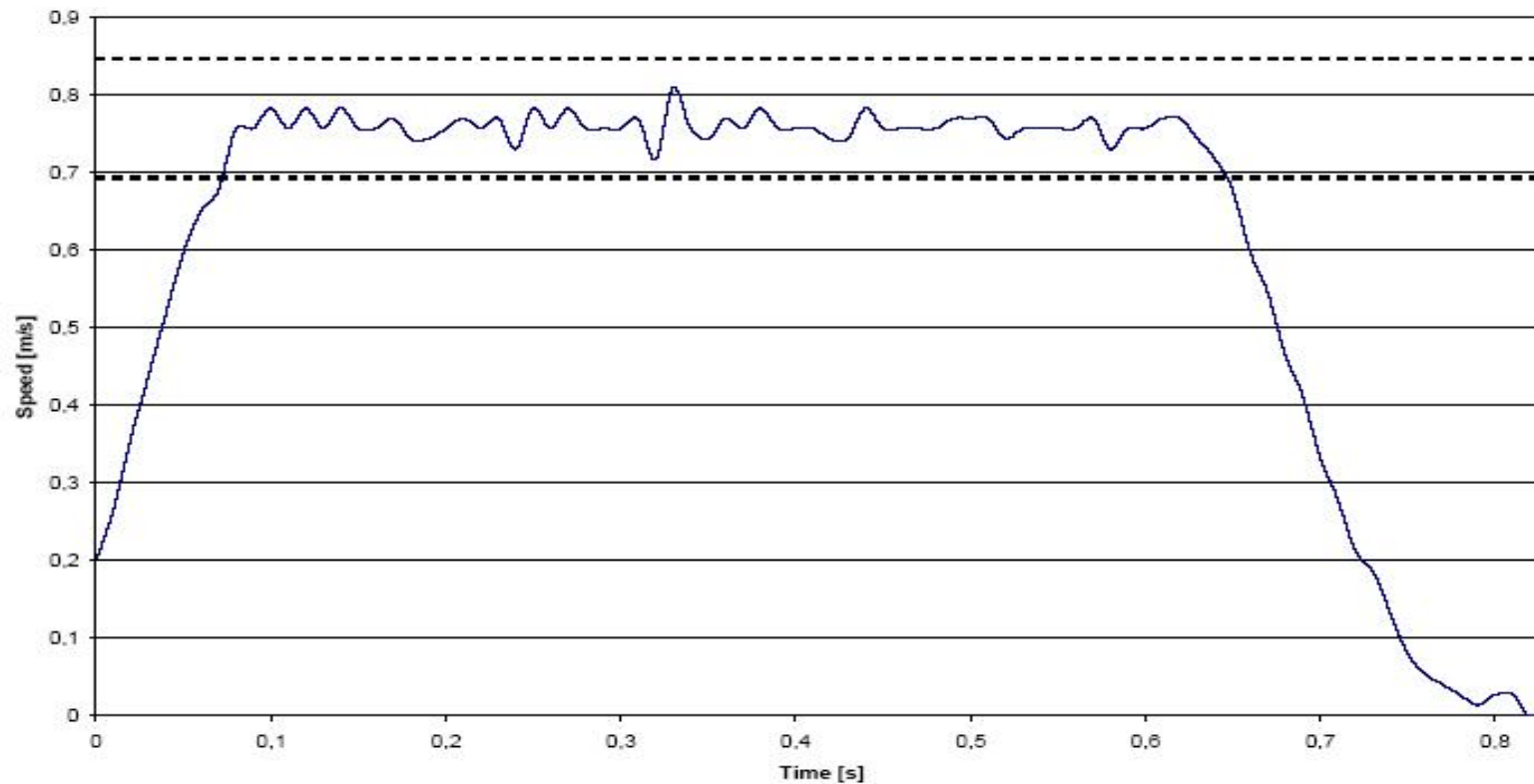


Figure 19: Speed measurement for the fast mode using state space controller

comparison PID and SS methods

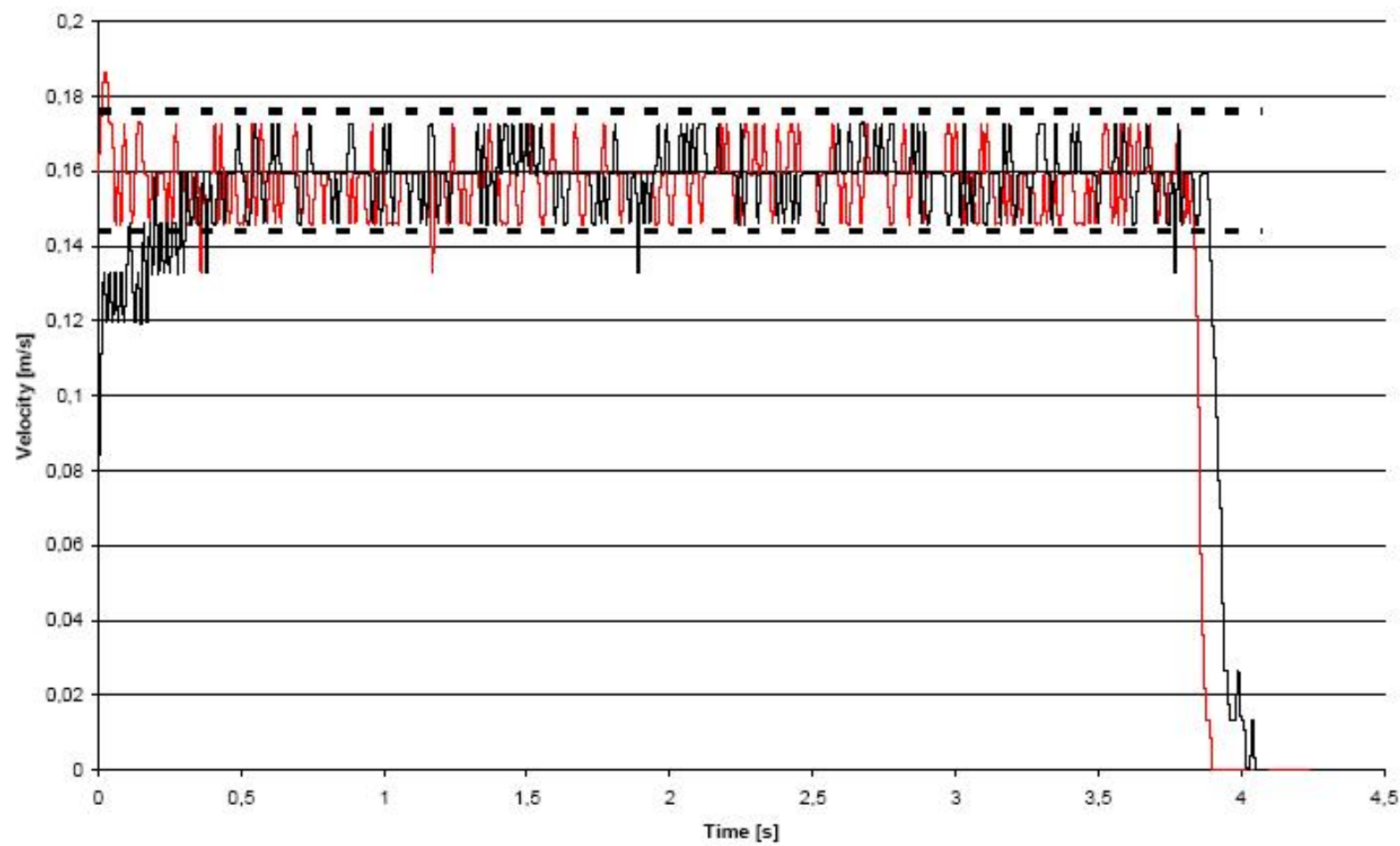


Figure 20: Speed measurements for the controlled fast mode and comparison with open-loop control

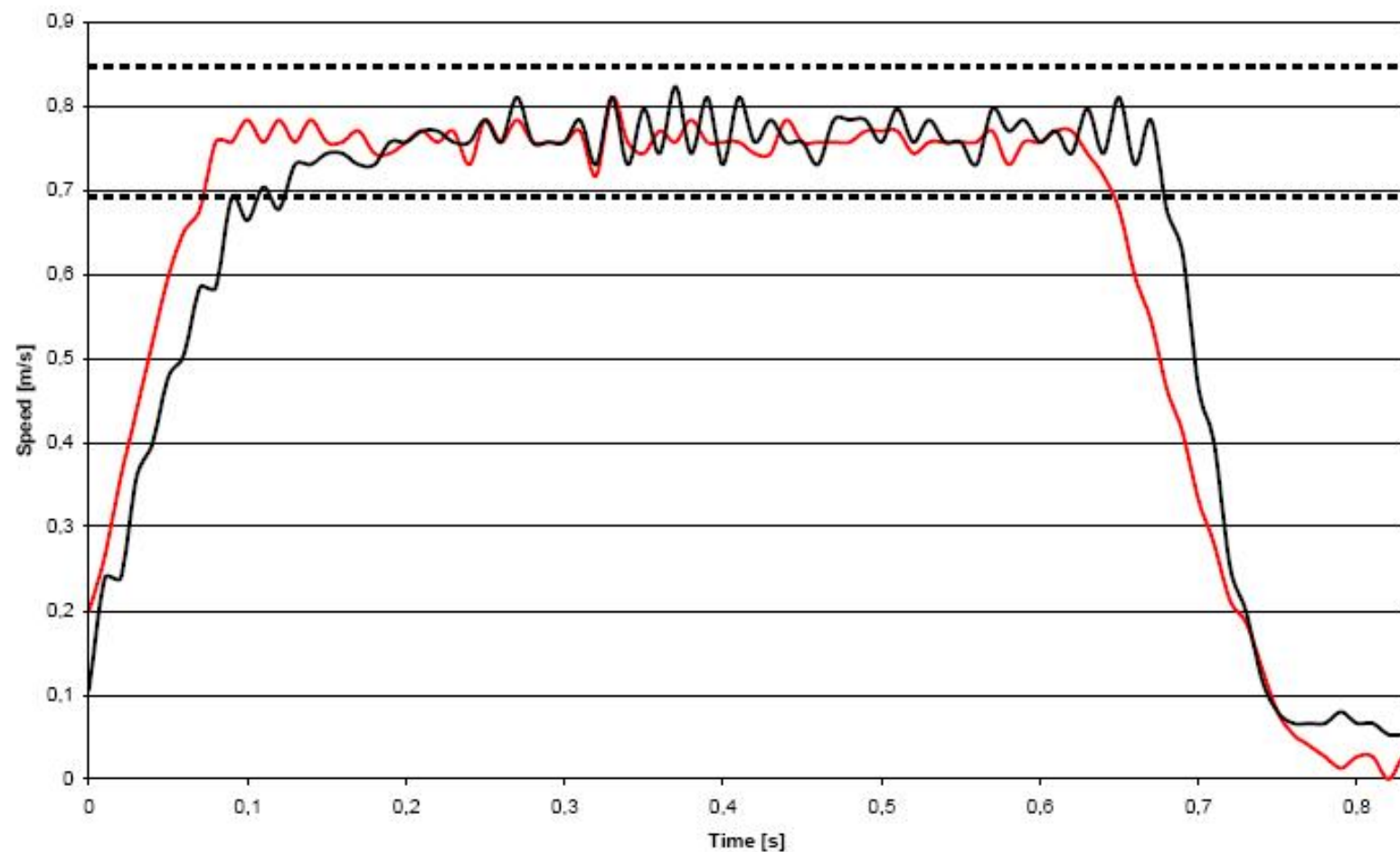


Figure 21: Speed measurements for the controlled fast mode and comparison with open-loop control

Conclusions

Mode-based control design for the BeoSound 9000 sledge system is discussed.

- The considered system is modeled according to first modeling principle. Then, system parameters are identified through experiments.
- Several control methods, namely digital PID, digital PI control with anti-windup, and observer-based state feedback with integral control, are developed and implemented into a microprocessor.
- The simulation and test results showed that both strategies of the digital PI control with anti-windup and the observer-based state feedback with integral control lead the controlled system to satisfy all demands defined by the industrial partner.